



**Black carbon over
the Himalayas and
Tibetan Plateau**

R. Zhang et al.

Quantifying sources, transport, deposition and radiative forcing of black carbon over the Himalayas and Tibetan Plateau

R. Zhang^{1,2,3}, H. Wang², Y. Qian², P. J. Rasch², R. C. Easter², P.-L. Ma², B. Singh², J. Huang¹, and Q. Fu^{1,3}

¹Key Laboratory for Semi-Arid Climate Change of the Ministry of Education, College of Atmospheric Sciences, Lanzhou University, Lanzhou 730000, Gansu, China

²Atmospheric Sciences and Global Change Division, Pacific Northwest National Laboratory (PNNL), Richland, WA 99352, USA

³Department of Atmospheric Sciences, Box 351640, University of Washington, Seattle, WA 98195, USA

Received: 25 October 2014 – Accepted: 9 December 2014 – Published: 7 January 2015

Correspondence to: H. Wang (hailong.wang@pnnl.gov)

Published by Copernicus Publications on behalf of the European Geosciences Union.

Title Page

Abstract

Introduction

Conclusions

References

Tables

Figures



Back

Close

Full Screen / Esc

Printer-friendly Version

Interactive Discussion



Abstract

Black carbon (BC) particles over the Himalayas and Tibetan Plateau (HTP), both airborne and those deposited on snow, have been shown to affect snowmelt and glacier retreat. Since BC over the HTP may originate from a variety of geographical regions and emission sectors, it is essential to quantify the source–receptor relationships of BC in order to understand the contributions of natural and anthropogenic emissions and provide guidance for potential mitigation actions. In this study, we use the Community Atmosphere Model version 5 (CAM5) with a newly developed source tagging technique, nudged towards the MERRA meteorological reanalysis, to characterize the fate of BC particles emitted from various geographical regions and sectors. Evaluated against observations over the HTP and surrounding regions, the model simulation shows a good agreement in the seasonal variation of the near-surface airborne BC concentrations, providing confidence to use this modeling framework for characterizing BC source–receptor relationships. Our analysis shows that the relative contributions from different geographical regions and source sectors depend on seasons and the locations in the HTP. The largest contribution to annual mean BC burden and surface deposition in the entire HTP region is from biofuel and biomass (BB) emissions in South Asia, followed by fossil fuel (FF) emissions from South Asia, then FF from East Asia. The same roles hold for all the seasonal means except for the summer when East Asia FF becomes more important. For finer receptor regions of interest, South Asia BB and FF have the largest impact on BC in Himalayas and Central Tibetan Plateau, while East Asia FF and BB contribute the most to Northeast Plateau in all seasons and Southeast Plateau in the summer. Central Asia and Middle East FF emissions have relatively more important contributions to BC reaching Northwest Plateau, especially in the summer. Although local emissions only contribute about 10% to BC in the HTP, this contribution is extremely sensitive to local emission changes. Lastly, we show that the annual mean radiative forcing (0.42 W m^{-2}) due to BC in snow outweighs the BC dimming effect (-0.3 W m^{-2}) at the surface over the HTP. We also find strong sea-

ACPD

15, 77–121, 2015

Black carbon over the Himalayas and Tibetan Plateau

R. Zhang et al.

Title Page

Abstract

Introduction

Conclusions

References

Tables

Figures



Back

Close

Full Screen / Esc

Printer-friendly Version

Interactive Discussion



Black carbon over the Himalayas and Tibetan Plateau

R. Zhang et al.

Title Page

Abstract

Introduction

Conclusions

References

Tables

Figures



Back

Close

Full Screen / Esc

Printer-friendly Version

Interactive Discussion



The HTP, often referred to as the Third Pole, has received much less scientific attention than the Polar Regions (Qiu, 2008), although it is the highest and largest plateau that stores one of the largest ice masses of the Earth system. The HTP also has a large area of seasonal and permanent snow cover and represents the most sensitive and visible indicator of climate change with its unique location for complex interactions among the atmosphere, hydrosphere and cryosphere (Pu et al., 2007; Xu et al., 2009; Yao et al., 2012). The glaciers and the associated snowmelt over the HTP, called the “World Water Tower”, have a great potential to modify the regional hydrology and to trigger natural hazards, which impact a large portion of the population in and around the region (Barnett et al., 2005; Singh and Bengtsson, 2004; Xu et al., 2008; Kaser et al., 2010; Immerzeel et al., 2010; Yao et al., 2012; Bolch et al., 2012). The HTP also exerts profound influences on atmospheric circulation patterns and climate through its significant mechanical and thermal effects due to its large area, highly elevated topography and geographical location in the Earth system (Yeh et al., 1957; Manabe and Terpstra, 1974; Ye and Gao, 1979; Yanai et al., 1992; Ye and Wu, 1998; Wu et al., 2012). In the winter, the HTP acts as a giant wall across the Eurasian continent that blocks cold outbreaks from high latitudes, and confines the winter monsoon to eastern and southern Asia (Wu et al., 2012). In the summer, the HTP serves as a huge heat source, with strong surface sensible heating and latent heating over central and eastern Plateau (Wu et al., 2012). The surface sensible heat flux over the HTP has weakened in recent decades, mainly due to global warming (Duan and Wu, 2008).

Under the background of global warming, the climate of the HTP is changing rapidly. Observational evidence indicates that the surface air temperatures on the HTP have increased about 1.8 °C over the past 50 years (Wang et al., 2008). Xu et al. (2009) reported that the large area at elevation above 4000 m has warmed at 0.3 °C per decade in the past three decades, which is twice the global average warming. The warming trend in the cold season was greater than that in the warm season (Zhao et al., 2004). A number of recent studies reported that the glaciers on the HTP have undergone widespread losses at an increasing rate in past decades (Qin et al., 2006; Li et al.,

Black carbon over the Himalayas and Tibetan Plateau

R. Zhang et al.

Title Page

Abstract

Introduction

Conclusions

References

Tables

Figures



Back

Close

Full Screen / Esc

Printer-friendly Version

Interactive Discussion



2008; Kang et al., 2010; Bolch et al., 2012) and have undergone accelerated retreat in recent years (Yao et al., 2007). The rapid warming and the accelerated glacier retreat have been primarily attributed to increasing greenhouse gases (GHGs) (Barnett et al., 2005; Duan et al., 2006; Ren et al., 2006), but other factors may be partly responsible for the accelerated warming over the HTP, such as atmospheric heating by absorbing aerosols, land use changes, and reduction of snow albedo induced by deposition of light-absorbing impurities on snow (Kang et al., 2000; Prasad and Singh, 2007; Ramanathan et al., 2007; Flanner et al., 2007, 2009; Yasunari et al., 2010; Xu et al., 2009; Qian et al., 2011, 2015). Lau et al. (2006, 2010) proposed and demonstrated the Elevated Heat Pump (EHP) mechanism, whereby heating induced by airborne BC and dust absorption can strengthen local circulations and lead to a northward shift of the monsoon rain belt, widespread enhanced warming over the HTP, and accelerated snowmelt and glacier retreat. Previous observational and modeling studies have indicated that BC deposition on snow and ice, which has a rapidly increasing trend, has been a significant contributor to the early snowmelt and rapid glacier retreat over the HTP (Flanner et al., 2007, 2009; Ming et al., 2008; Xu et al., 2009; Kaspari et al., 2011; Menon et al., 2010; Qian et al., 2011, 2015; Lu et al., 2012; M. Wang et al., 2014). Flanner et al. (2007) found that the largest regional annual mean forcing due to BC in snow is located in the HTP. Xu et al. (2009) and Lau et al. (2010) suggested that the BC in snow/ice may be partly responsible for the observed acceleration of glacier retreat in the HTP. Qian et al. (2011) showed that the snow albedo effect of BC is more efficient in accelerating snowmelt (i.e., reducing snow cover and snow water) than warming in the atmosphere induced by greenhouse gases.

Global warming, glacier retreat and snow-cover reduction have been projected to accelerate throughout the 21st century (IPCC, 2013). Understanding the role of BC in this is becoming increasingly important. A large fraction of BC in the Earth system originates from anthropogenic activities. Reduction of emissions from BC-rich sources represents a potential mitigation strategy to manage the road map of climate forcing because BC has a positive radiative forcing but a short atmospheric lifetime (Bond et al.,

Black carbon over the Himalayas and Tibetan Plateau

R. Zhang et al.

[Title Page](#)[Abstract](#)[Introduction](#)[Conclusions](#)[References](#)[Tables](#)[Figures](#)[Back](#)[Close](#)[Full Screen / Esc](#)[Printer-friendly Version](#)[Interactive Discussion](#)

2013). Since BC over the HTP may originate from a variety of geographical regions and emission sectors, it is essential to quantify the source–receptor relationships of BC in order to understand the contributions of open fire and anthropogenic emission sectors to BC over the HTP. This exercise is also essential to provide guidance for potential mitigation actions.

Many factors can affect the amount and impacts of BC on the HTP region, including the distance from source to the HTP, meteorological conditions that determine the transport pathways and clouds/precipitation along the pathways, and physical and chemical properties of the mixture of BC and other aerosol species that influence the interactions with clouds and subsequent wet removal during the transport. Some studies have used the back-trajectory approach to identify possible source regions for both airborne BC and that deposited on snow and ice, by tracking air mass reaching sampling sites over the HTP (e.g., Ming et al., 2008, 2009; Cao et al., 2009; Bonasoni et al., 2010; Zhao et al., 2013; Zhang et al., 2013). Lu et al. (2012) developed a novel back-trajectory approach to also account for emissions, transformation/aging and removal processes of BC. Kopacz et al. (2011) attempted to provide the spatially and seasonally resolved source contributions to the BC atmospheric column burden above five glaciers across the HTP in 2001, using a global chemical transport model.

In this study, we use an aerosol-climate model with a newly developed explicit source tagging approach (H. Wang et al., 2014) to produce a detailed characterization of the fate of BC emitted from various geographical regions and sectors (e.g., fossil fuel, biofuel and biomass burning emissions) and transport pathways to the HTP. Section 2 describes the model and methods used in this study. Section 3 presents an evaluation of modeled BC surface concentrations and seasonal snow cover over the HTP region. The transport pathways and source attribution results are presented in Sect. 4. The radiative effects of BC in the atmosphere and of both BC and mineral dust in snow are compared in Sect. 5, followed by the summary and conclusions in Sect. 6.

Black carbon over the Himalayas and Tibetan Plateau

R. Zhang et al.

[Title Page](#)[Abstract](#)[Introduction](#)[Conclusions](#)[References](#)[Tables](#)[Figures](#)[Back](#)[Close](#)[Full Screen / Esc](#)[Printer-friendly Version](#)[Interactive Discussion](#)

removal of aerosols. We use the NASA Modern Era Retrospective-Analysis for Research and Applications (MERRA) reanalysis dataset (Rienecker et al., 2011), using a horizontal resolution of $1.9^\circ \times 2.5^\circ$ and 56 vertical levels. The goal is to characterize the fate of BC emitted from various geographical regions and sectors, their transport pathways to the HTP, and their radiative forcing with seasonal variations. The simulation is performed for year 2001 with prescribed sea surface temperatures. Kopacz et al. (2011) quantified the contributions of spatially and seasonally resolved sources of BC to the atmospheric column burden above five glaciers across the HTP using the adjoint method of the GEOS-Chem (Goddard Earth Observing System-Chemistry) model for the same year 2001.

2.2 BC source regions and sectors

BC emission datasets have large uncertainties (e.g., Bond et al., 2013), and there are different inventories available for climate modeling. We use the present-day (i.e., year 2000) monthly mean emission inventories for BC provided by Lamarque et al. (2010). They were built for the climate model simulations in the Coupled Model Intercomparison Project Phase 5 (CMIP5) (Taylor et al., 2012) performed for the fifth assessment report (AR5) of the Intergovernmental Panel on Climate Change (IPCC). The AR5 BC emissions being used in our CAM5 simulation include monthly varying elevated open fire emissions (injection altitude up to 6 km), and yearly constant surface emissions from shipping and from six sectors over land: agricultural waste burning, domestic, energy, industry, transportation, and waste treatment. To prepare for the BC source sector tagging, we divide the total surface emissions into two broader sectors, biofuel and fossil fuel, by using the ratio of biofuel to biofuel plus fossil fuel at each model grid provided by Dentener et al. (2006). We then combine the biomass burning (open fire) emissions and surface biofuel emissions, hereafter, referred to as BB (biofuel and biomass) sector. The shipping emissions are combined with the fossil fuel emissions over land to form the FF (fossil fuel) sector.

Black carbon over the Himalayas and Tibetan Plateau

R. Zhang et al.

Title Page

Abstract

Introduction

Conclusions

References

Tables

Figures



Back

Close

Full Screen / Esc

Printer-friendly Version

Interactive Discussion



Sixteen geographical BC source regions (Fig. 1a) are defined using the definition of source/receptor regions by Work Plan (WP 2.1) of the Task Force on Hemispheric Transport of Air Pollution (<http://iek8wikis.iek.fz-juelich.de/HTAPWiki/WP2.1>). They are ARC (Arctic), NAM (North America), CAM (Central America), SAM (South America), EUR (Europe), NAF (North Africa), SAF (South Africa), MDE (Middle East), CAS (Central Asia), SAS (South Asia), EAS (East Asia), SEA (South East Asia), PAN (Pacific, Australia and New Zealand), RBU (Russia, Belarus and Ukraine), HTP (Himalayas and Tibetan Plateau) and ROW (Rest of World).

Figure 1b and Table S1 in the Supplement summarize the fractional contributions of BC emissions from the different source regions and sectors. The global annual mean BC emission rate is 7.78 Tgyr^{-1} , with 56.2 % (sum of the red bars) from BB emissions (33.6 % from fires and 22.6 % from biofuel) and 43.8 % (sum of the blue bars) from FF emissions. The two largest contributors are BB emissions from SAF (about 20 %) and FF emissions from EAS (about 15 %), followed by BB emissions from SEA (7.7 %), EAS (6.4 %), SAS (6.2 %) and SAM (5.7 %), and EUR FF (6.4 %) emissions. The geographical distributions of BC annual mean emission fluxes from BB and FF sectors for year 2000 are shown in Fig. S1 (in Supplement).

We use two metrics for quantifying source–receptor relationships and the sensitivity of BC in a receptor region to various sources following H. Wang et al. (2014), but we extend them to treat BB and FF sectors separately.

1. The fractional contribution of BB and FF emissions from source region i to a BC property in the receptor region (HTP), C_i^{BB} or C_i^{FF} , is defined as

$$C_i^{\text{BB}} = \frac{A_i^{\text{BB}}}{\sum_{i=1}^N (A_i^{\text{BB}} + A_i^{\text{FF}})} \quad C_i^{\text{FF}} = \frac{A_i^{\text{FF}}}{\sum_{i=1}^N (A_i^{\text{BB}} + A_i^{\text{FF}})}$$

Where A_i^{BB} and A_i^{FF} are a BC property (e.g., mass mixing ratio, column burden, or deposition flux) in/over the receptor region resulting from BB and FF emissions,

Black carbon over the Himalayas and Tibetan Plateau

R. Zhang et al.

Title Page

Abstract

Introduction

Conclusions

References

Tables

Figures



Back

Close

Full Screen / Esc

Printer-friendly Version

Interactive Discussion



respectively, in source region i . The summation $\sum_{i=1}^N (A_i^{\text{BB}} + A_i^{\text{FF}})$ represents the total BC from all source regions ($N = 16$ in this study) and sectors (BB and FF). Note that for BC properties such as column burden, surface mixing ratio, and deposition flux, the tagging method in CAM5 explicitly calculates how much is due to emissions from each source region and sector.

2. Efficiency of BB and FF emissions from source region i in changing BC in a receptor region is defined as

$$S_i^{\text{BB}} = \frac{C_i^{\text{BB}}}{\left[\frac{E_i^{\text{BB}}}{\sum_{i=1}^N (E_i^{\text{BB}} + E_i^{\text{FF}})} \right]} \quad S_i^{\text{FF}} = \frac{C_i^{\text{FF}}}{\left[\frac{E_i^{\text{FF}}}{\sum_{i=1}^N (E_i^{\text{BB}} + E_i^{\text{FF}})} \right]}$$

Where C_i^{BB} and C_i^{FF} are the fractional contribution, E_i^{BB} and E_i^{FF} are the total BB and FF emission rates, respectively, in source region i . The summation $\sum_{i=1}^N (E_i^{\text{BB}} + E_i^{\text{FF}})$ represents the global total emission rate. The efficiency metric S_i^{BB} or S_i^{FF} also characterizes the sensitivity of aerosol properties in the receptor region to per unit (BB or FF) emissions in the source region.

3 Model evaluation against available observations

The CAM5 model has been evaluated in detail from different perspectives with available observations such as aerosol mass concentration, aerosol number concentration and size distribution, aerosol optical properties, cloud properties, aerosol deposition and BC in snow over various regions in previous studies (Liu et al., 2012; H. Wang et al., 2013; Ma et al., 2013; Jiao et al., 2014; Lee et al., 2013; Qian et al., 2014). Because of the complex topography and meteorology of the HTP and the relatively coarse resolution of global model, further model evaluation focusing on the HTP region is critical. Here we use near-surface atmospheric BC concentrations measured at a few HTP sites and

the snow cover fraction retrieved from satellite to evaluate the CAM5 performance in the HTP.

3.1 Atmospheric BC surface concentration

There are seven remote sites that have surface measurements of seasonal BC aerosol concentrations available. The locations and elevations of the sites and the sampling time periods and observation methods are described in Table 1. Figure 2 shows the comparison of seasonal mean BC concentrations between observations and CAM5 results. Note that model results represent mean concentrations in the grid box that the sampling sites reside in and at the grid-mean elevation, which could deviate significantly from the sampling point near complex terrain. All sites have non-negligible amounts of BC in the near-surface air. The error bars indicate the intra-seasonal and inter-annual variations if multi-year data were used for given season and site. However, the uncertainties of observed BC surface concentrations mainly originate from the large discrepancies between different measurement methods, the mixing of BC with other components (e.g., organic carbon and mineral dust) in the aerosol samples, and the sampling time and location (Bond et al., 2013; Petzold et al., 2013). BC surface concentrations over the various sites show strong seasonal variations, which are reasonably captured by the model. The modeled magnitude of BC concentrations has a good agreement with observations at some sites (e.g., Fig. 2b, d and g), but the model clearly overestimates BC at the Muztagh Ata site (Fig. 2a) and underestimates at the Lulang site (Fig. 2e). The large underestimation (about 1000 m; see Table 1) of the Muztagh Ata site elevation in the model, determined by the model grid resolution, could largely explain the overestimation of BC since BC concentrations have sharp decreases with height in this region. At the sites over southern HTP (i.e., Hanle, Manora Peak, NCO-P, Lulang and NCOS), the BC surface concentrations in the summer (JJA) are lower, mainly due to wet scavenging by more frequent precipitation and partly due to the minimal emissions from domestic heating and wildfires over Himalaya foothills and Indo-Gangetic Plains (IGP) during the Indian summer monsoon season (Marinoni

Black carbon over the Himalayas and Tibetan Plateau

R. Zhang et al.

Title Page

Abstract

Introduction

Conclusions

References

Tables

Figures



Back

Close

Full Screen / Esc

Printer-friendly Version

Interactive Discussion



year 2001 in all seasons except for JJA, when SCF is notably higher over northwest Plateau for the climatology that included June SCF in the average. On average, SCF is about 5 % higher in June than in July and August.

There are strong spatial and seasonal variations in SCF due to the complex terrain and seasonal variation in snowfall and melting. The SCF over the entire HTP reaches the maximum in the winter (DJF), while decreases to almost none (less than 5 %) in July and August. Snow covers the western and southeastern Plateau during the transition seasons (MAM and SON). The CAM5 simulation shows a good agreement with MODIS in the annual mean (ANN) SCF and the strong seasonality. The most persistent snow cover at the southern and western edges of the HTP and the relatively less persistent in the HTP interior are captured by the CAM5 model. The performance of the CAM5 has been dramatically improved, in comparison to its earlier version (CAM3) that remarkably overestimated the SCF especially over the HTP interior (Qian et al., 2011), although the CAM5 still overestimates the SCF in the western Plateau in DJF and MAM and underestimates it in JJA.

Although we believe that the CAM5 SCF biases are qualitatively robust, it is worth noting that the MODIS products have uncertainties as well. Pu et al. (2007) evaluated the MODIS SCF products over the HTP against ground-based snow observations and showed that total error in MODIS SCF products over the HTP is about 10 %. However, their analysis based on MODIS eight-day snow-cover composite gave a significantly higher SCF (more than 10 %) than the one we show here using daily products, especially, in winter and early spring. Interestingly, based on a different source of observation, Qin et al. (2006) found that snow covers about 59 % of the Tibetan Plateau in winter, which is very close to the mean SCF in our CAM5 simulation. Nonetheless, we keep this discrepancy in mind when interpreting the wintertime BC-in-snow radiative forcing that suffers the most from such potential SCF bias.

Black carbon over the Himalayas and Tibetan Plateau

R. Zhang et al.

Title Page	
Abstract	Introduction
Conclusions	References
Tables	Figures
◀	▶
◀	▶
Back	Close
Full Screen / Esc	
Printer-friendly Version	
Interactive Discussion	



4 Modeled transport pathways and source attribution of BC in the HTP

4.1 Transport pathways

The direct source tagging method can clearly characterize the three-dimensional transport pathways of BC emitted from various source regions and sectors to the HTP receptor region. General circulation patterns over the HTP and surroundings are typically affected by mid-latitude westerlies in the winter and Asian monsoon in the summer, including the South Asian summer monsoon and East Asian summer monsoon (Xu et al., 2009; Yao et al., 2012; Wu et al., 2012; also see Fig. S2).

Figure 4 illustrates circulation patterns over HTP and BC transport pathways from six major source regions to the HTP in the winter (DJF) and summer (JJA). (See similar plots in Figs. S3–S5 for other tagged source regions.) In the winter, the strong surface cooling over the HTP leads to subsidence/divergence and the formation of an enhanced local circulation cell, while in the summer air converges toward the HTP from the surroundings, particularly from the South Asia, due to the ascending of strongly heated air over the HTP (e.g., Wu et al., 2012), as also indicated by the arrows in the vertical cross-sections in Fig. 4. In the winter, the subtropical westerlies extend to about 10° N in mid-/upper troposphere and 20° N near surface, and the tropical easterlies are weak (see the white contours of latitude-height cross-section panels in Fig. 4). The circulation patterns near the HTP change dramatically during the summer monsoon season. The reversal of surface wind regime in the tropics (e.g., Arabian Sea, Bay of Bengal, and South China Sea) is characteristic of the Asian summer monsoon climate (see Fig. S2e and g). The subtropical westerlies recede to north of 30° N and the center of the westerly jet shifts to about 40° N in JJA (from about 30° N in DJF). The strong easterlies characterize the upper troposphere of tropical region (south of HTP), while the southwesterly flow prevails in the lower troposphere (white contours of latitude-height cross-section panels in Fig. 4). The prevailing winds during the transition seasons (MAM and SON) between DJF and JJA are still westerlies (Fig. S2b and d).

Black carbon over the Himalayas and Tibetan Plateau

R. Zhang et al.

Title Page

Abstract

Introduction

Conclusions

References

Tables

Figures



Back

Close

Full Screen / Esc

Printer-friendly Version

Interactive Discussion



deposition rate over the HTP and five sub-regions. The seasonal variation of the ratio of wet to total BC deposition is superimposed. The Central Plateau is the cleanest region during all seasons, compared to other sub-regions in the HTP (Fig. 5e). Both BC column burden and deposition rate from the BB sector peak in MAM over the HTP, mostly in the Himalayas and Southeast Plateau region. The FF BC burden in the HTP peaks in the summer mainly due to the seasonal maximum over Northwest and Northeast Plateaus. However, BC wet removal rate over the Northwest Plateau is at minimum in the summer, as opposed to the summer maximum in other sub-regions and the entire HTP region. For Himalayas, Southeast and Central Plateau, the seasonal variation (i.e., maximum in MAM followed by a sharp decrease to JJA) of BB and FF column burden (Fig. 5c–e) is similar to the variation of observed surface concentrations at sites located in these sub-regions (Fig. 2b and d–f). In the Himalayas and Southeast Plateau, the ratio of BC column burden to deposition rate (Fig. 5c and d), indicator of removal time scale or lifetime, is the smallest (less than 1 day) during the Asian summer monsoon (JJA) due to the efficient wet scavenging of BC by abundant precipitation. In Northwest and Northeast Plateau, the BC column burden increases from DJF to JJA and reaches the maximum in JJA, and then decreases in SON (Fig. 5b and f), partly due to the peak contribution of EAS and CAS emissions in JJA. This trend is also similar to that in the observed surface concentrations (Fig. 2a and g). The deposition rate follows the same seasonal variation of column burden over the Northeast Plateau, while the deposition has a minimum in JJA over the Northwest Plateau when the column burden is at maximum likely due to the less efficient wet removal in this region (Fig. 5b and f).

The annual mean BC column burden over the HTP has almost the same contributions from BB and FF emission origins, with BB dominating in DJF and MAM and FF in JJA. In the Himalayas, BC is predominantly from BB sector for all seasons (Fig. 5c). In the Southeast and Central Plateaus, the dominant source sector is BB in DJF and MAM, but FF dominates in JJA. The dominant source sector over the Northwest and Northeast Plateaus is always FF, especially in the summer. We need to analyze the

Black carbon over the Himalayas and Tibetan Plateau

R. Zhang et al.

Title Page

Abstract

Introduction

Conclusions

References

Tables

Figures



Back

Close

Full Screen / Esc

Printer-friendly Version

Interactive Discussion



source–receptor relationships in order to quantify the roles of BB and FF emissions from the various source regions in determining BC over the HTP and the sub-regions.

4.3 BC source–receptor relationships

Our analysis shows that the relative contributions to BC from different source regions and sectors depend on seasons and the locations in the HTP. As shown in Fig. 6, the largest contribution to the annual mean BC burden and surface deposition for the entire HTP region is from BB emissions from SAS, followed by FF emissions from SAS and then the FF from EAS. The same roles hold for all the seasonal means except for the summer (JJA) when the EAS FF becomes more important for BC column burden in the HTP and, to a lesser extent, for deposition.

The SAS emissions account for 50% of the annual mean burden over the HTP, including 33% from BB and 17% from FF. The other 50% is mostly from the EAS (5% BB and 14% FF), HTP (6% BB and 6% FF), CAS FF (4%), MDE FF (4%) and SAF BB (3%). The source attribution for annual mean BC deposition for the entire HTP is similar, but SAS contributes even more to BC deposition than to the column burden.

BC annual mean burden over the HTP has nearly equal contributions from BB and FF emissions. However, contribution by BB emissions, mainly from SAS, is larger than from FF sector in DJF and MAM. In the summer (JJA), the largest contribution (about 29%) to HTP BC is from EAS FF emissions. This is partly due to the change of circulation patterns (Fig. 4) and effective wet removal of SAS BB emissions. Note that EAS FF emissions are much larger than FF emissions from any other of the source regions, and are more than twice the EAS BB emissions.

For BC in the five finer receptor regions of interest (as defined in Fig. 5g), SAS BB and FF have the largest contribution to BC in Himalayas and Central Plateau, while EAS FF and BB contribute the most to Northeast Plateau in all seasons and Southeast Plateau in the summer. Central Asia and Middle East FF emissions have relatively more important contribution to BC reaching Northwest Plateau, especially in the summer.

Black carbon over the Himalayas and Tibetan Plateau

R. Zhang et al.

Title Page

Abstract

Introduction

Conclusions

References

Tables

Figures



Back

Close

Full Screen / Esc

Printer-friendly Version

Interactive Discussion



Black carbon over the Himalayas and Tibetan Plateau

R. Zhang et al.

Title Page

Abstract

Introduction

Conclusions

References

Tables

Figures



Back

Close

Full Screen / Esc

Printer-friendly Version

Interactive Discussion



For the Northwest Plateau (Fig. 6b), the prevailing winds in this sub-region are west-
erly throughout the year (Fig. S2; Cao et al., 2009; Xu et al., 2009), so the important
source regions ought to locate at the west of HTP (e.g., MDE, EUR, and parts of SAS
and RBU in Fig. 1a). SAS emissions are still the dominant source for the annual BC
burden in this sub-region (17% from BB and 14% from FF), followed by HTP local
emissions (9% from BB and 13% from FF), CAS (2% from BB and 14% from FF),
MDE FF (8%) and EAS FF (7%). BC emissions from SAS are the dominant source
in DJF, MAM and SON. CAS becomes the dominant source region (5% from BB and
26% from FF) in JJA, even though CAS is not a significant emission source region
on a global basis (Fig. 1b). BC emitted from MDE is predominantly in the FF sector
throughout the year. Emissions from the rest of the tagged sources (in addition to the
top six) become more significant in this sub-region (black color in Fig. 6b), mostly from
EUR and RBU through long-range transport (Fig. S3). The source attribution for BC de-
position in this sub-region is similar to that of the column burden, but BC emitted from
SAS and MDE appears to be more efficient in deposition except for the JJA season
when BC from EAS contributes more to deposition than to column burden.

The Himalayas sub-region located along the southern edge of the HTP is in close
proximity to the SAS. Thus emissions from SAS are absolutely the dominant source
for BC in Himalayas throughout the year. This sub-region receives more BC from BB
sector than FF because BC emissions in SAS are mainly in the BB sector, especially in
MAM season (Figs. 1b and S6). For the annual mean burden, BC from SAS contributes
81% (54% from BB and 27% from FF), followed by HTP local emissions (6% from BB
and 3% from FF). It is worth noting that SAF BB emissions contribute about 10% to
burden in DJF through a long-range transport. BC deposition in this sub-region also
predominantly originates from SAS, which is consistent with previous studies by Ming
et al. (2008) and Kopacz et al. (2011).

For the Southeast Plateau (Fig. 6d), the BC source contribution profile is similar to
that of Himalayas during DJF and MAM season, in which SAS is still the dominant
source, especially in MAM (74% contribution to column burden, including 53% from

Black carbon over the Himalayas and Tibetan Plateau

R. Zhang et al.

Title Page

Abstract

Introduction

Conclusions

References

Tables

Figures



Back

Close

Full Screen / Esc

Printer-friendly Version

Interactive Discussion



BB and 21 % from FF), although the contribution from EAS is larger here than for the Himalayas. As also pointed by Ramanathan et al. (2007), BC over the SAS can be transported to the Southeast Plateau by the southern branch of the westerlies during the winter and spring. However, the BC source contribution profile changes dramatically during the summer when emissions in EAS become the dominant source to this sub-region (68 % to column burden, including 23 % from BB and 45 % from FF). Kopacz et al. (2011) also found that the BC from south-eastern China is the dominant contributor to the Southeast Plateau in July. For the annual mean burden in this sub-region, SAS is still the dominant contributor (40 % from BB and 17 % from FF), followed by EAS (8 % from BB and 15 % from FF), HTP (6 % from BB and 6 % from FF). BC originating from EAS contributes more to deposition than to burden in this sub-region.

For the Central Plateau (Fig. 6e), source attribution profiles for annual and seasonal BC are very similar to those of the entire HTP region with SAS being the dominant source region throughout the year except that EAS has comparable contributions in JJA. Ming et al. (2010) pointed out that pollutants from the Indo-Gangetic Basin could be transported to the Central Plateau by both the summer monsoon and the westerlies. Xia et al. (2011) also found that the substantial regional atmospheric brown haze from the nearby regions of SAS is the main source for the background aerosols in the Central Plateau based on sunphotometer and satellite observations.

Compared to the other sub-regions, the Northeast Plateau receives the largest contribution of BC from EAS throughout the year (50 % to annual mean burden, including 12 % from BB and 38 % from FF; see Fig. 6f), especially in JJA (17 % from BB and 49 % from FF). The EAS FF sector contribution and the magnitude of burden (Fig. 5f) over the Northeast Plateau have strong seasonal variations, mostly due to variations in meteorology because the FF emissions in our simulation do not vary seasonally. Kopacz et al. (2011) indicate that the primary contribution to BC over the Northeast Plateau is from western China during January and April (transported by mid-tropospheric westerlies), and from central-eastern China during July and October (transported by boundary layer flow). Other main contributions to BC burden over the Northeast Plateau include

13% from SAS and 10% from HTP local emissions. Similar to the Northwest Plateau, some other upwind source regions (e.g., CAS, MDE, RBU and EUR) have a significant contribution to the Northeast sub-region as well.

4.4 Seasonal variation of HTP BC sensitivity

5 Following H. Wang et al. (2014), we defined the “efficiency” metric in Sect. 2.2 to quantify the sensitivity of BC relative response to per unit perturbation of emissions in different source regions. This metric has the value of 1 if the entire globe is treated as a single source region, so we may assume the global mean efficiency of 1 as a reference to measure the sensitivity to perturbation from different source regions/sectors.

10 Figure 7 shows efficiencies of tagged sources in affecting the BC seasonal and annual mean column burden and deposition in the HTP and five sub-regions (as defined in Fig. 5g). BC in the same receptor regions is generally most sensitive to change in local emissions, regardless of seasons, emission sectors and locations of receptor regions. Among all the source regions, although the HTP local (FF + BB) emissions only contribute about 10%, BC in the HTP is extremely sensitive to changes in the emissions within HTP. In addition to the local emissions, BC in the HTP is also sensitive to emissions in neighboring source regions (e.g., SAS and CAS) and emissions from distant sources such as MDE. Not only does the SAS have large contribution to BC burden and deposition over the HTP, as well as most of the sub-regions except for the
15 Northeast Plateau (receptor V), but also the efficiencies for SAS emissions are high for almost all of the sub-regions especially the Himalayas (receptor II). BC in the Northeast Plateau (receptor V) is quite sensitive to EAS emissions in all seasons, while BC in the Southeast Plateau is sensitive to EAS emissions in JJA and SON. Although BC emissions from MDE and CAS are weak (Fig. 1b) and their contributions to the HTP
20 are relatively low, their efficiencies are high. BC over Northwest Plateau (receptor I) and Central Plateau (receptor IV) is extremely sensitive to emissions from CAS in JJA. These source–receptor relationships of sensitivity will provide useful information for

Black carbon over the Himalayas and Tibetan Plateau

R. Zhang et al.

Title Page

Abstract

Introduction

Conclusions

References

Tables

Figures



Back

Close

Full Screen / Esc

Printer-friendly Version

Interactive Discussion



policymakers to improve the effective mitigation road map in order to potentially slow down the glacier retreat in the HTP region.

5 Radiative forcing

The BC-in-snow effect can be quantified using the online calculation of radiative forcing in the SNICAR (Snow, Ice, and Aerosol Radiative) model (Flanner et al., 2007) coupled to CAM5, and then compared to airborne BC radiative forcing. Figure 8 shows seasonal and annual mean BC all-sky shortwave direct radiative forcing (DRF) at the surface (dimming) and the top of the atmosphere (TOA), and the BC-in-snow radiative forcing (darkening) averaged over the entire HTP and the five sub-regions (as defined in Fig. 5g). Note that the BC-in-snow forcing is averaged over all model grids in the area (i.e., zero enters the calculation for any grid when snow is not present). The radiative forcing of BC (and dust) in snow is small in JJA and SON due to a lack of snow cover (Fig. 3). The forcing maximum occurs during the spring melt (MAM) when the insolation is rather intense and BC accumulates at the surface of the snowpack as the snow melts (Conway et al., 1996; Flanner et al., 2007, 2009), and when the snow-albedo feedback is strongest (Hall and Qu, 2006). This strong seasonal variation also explains why the coefficient of variation (i.e., the ratio of the SD to the mean) is greater than 1 for the annual mean BC-in-snow forcing over the entire HTP and all sub-regions. The seasonal variations of airborne BC DRF at the TOA and surface are consistent with that of the BC column burden (Fig. 5). For the entire HTP (Fig. 8a1), the annual mean surface radiative forcing due to BC in snow (0.42 W m^{-2}) exceeds the BC dimming effect at the surface (-0.3 W m^{-2}). The annual mean BC-in-snow forcing is even higher over the Northwest Plateau (Fig. 8b1) and Himalayas (Fig. 8c1), and far exceeds the other forcings in the same sub-regions, although the BC-in-snow effect may be over-estimated due to the potential positive bias in snow cover fraction in our simulation (Fig. 3). The annual mean BC surface dimming exceeds the BC-in-snow effect in the Southeast (Fig. 8d1), Central (Fig. 8e1) and Northeast Plateau (Fig. 8f1). The minima

Black carbon over the Himalayas and Tibetan Plateau

R. Zhang et al.

Title Page

Abstract

Introduction

Conclusions

References

Tables

Figures



Back

Close

Full Screen / Esc

Printer-friendly Version

Interactive Discussion



of all BC-related forcings appear in the Central Plateau where the BC burden and deposition are the lowest among all the sub-regions (Fig. 5), and the SCF is very small (Fig. 3).

We have also calculated an approximate source attribution for the BC-in-snow radiative forcing over the HTP and its sub-regions, using the tagged-source BC deposition, which is simply assumed to be linearly proportional to BC-in-snow radiative forcing. The SCF is taken into account in the calculation (i.e., the deposition at each model grid is multiplied by SCF when calculating the area-average deposition). Overall, despite small quantitative differences, the source contributions to BC-in-snow forcing are similar to those for BC deposition (Fig. 6). The SAS BB emissions contribute the most to annual mean forcing over the HTP and sub-regions except for the Northeast Plateau that is mostly contributed by EAS FF emissions. During the winter and spring seasons over Northwest Plateau and Himalayas, when and where the forcing is the largest, SAS (especially the BB sector) is the major contributor.

Dust is a major contributor to the total aerosol burden over the HTP (e.g., Zhang et al., 2001). Although we don't focus on other snow impurities such as mineral dust, it is worth noting that dust-in-snow radiative forcing has been considered in our model simulation and it could be an important forcing agent. We also plotted dust-in-snow forcing over the HTP and sub-regions in Fig. 8 (along with the BC-induced forcings). The annual mean dust-in-snow forcing (0.33 W m^{-2}) is comparable to all of the other forcings over the HTP, especially in the springtime when dust outbreaks and can be transported to the HTP from the surrounding sources such as Taklimakan and Gobi deserts (Liu et al., 2008). The annual mean dust-in-snow forcing is as large as 0.99 and 0.59 W m^{-2} in the Northwest and Northeast Plateau, respectively (Fig. 8b1 and f1), which is in close proximity to the Taklimakan Desert (Huang et al., 2007; Chen et al., 2013), but negligibly small in the Southeast Plateau and Central Plateau. In the winter, the dominant dust in snow effect over Northeast Plateau is consistent with the recent observations. Huang et al. (2011), X. Wang et al. (2013) and Zhang et al. (2013)

Black carbon over the Himalayas and Tibetan Plateau

R. Zhang et al.

[Title Page](#)[Abstract](#)[Introduction](#)[Conclusions](#)[References](#)[Tables](#)[Figures](#)[Back](#)[Close](#)[Full Screen / Esc](#)[Printer-friendly Version](#)[Interactive Discussion](#)

found that insoluble light-absorbing particles in snow are dominated by local soil and desert dust in the Qilian Mountain (Northeast Plateau).

Both snow cover fraction (SCF) and mass concentration of snow impurities affect the calculation of radiative forcing in snow. We have evaluated the model estimation of SCF in different seasons (Fig. 3). We have also compared BC concentration and deposition flux from our model results to a recent modeling study by Ménégoz et al. (2014) and to observations in the HTP (Ginot et al., 2014) (Table S2). Bond et al. (2013) pointed out that observations of BC in snow pits or ice cores mostly involve snow/ice samples obtained in the summer and early fall, when almost all grid boxes the sample sites located in are snow free in the HTP. They also indicated that the CAM3 global climate model (Flanner et al., 2009) may be overestimating snow BC concentrations in the HTP, especially in the spring. Our comparison shows that despite a smaller bias than in Ménégoz et al. (2014) the CAM5 model still largely overestimates BC concentrations in snow but underestimates dust concentrations in snow over the HTP. Ménégoz et al. (2014) provided a few possible reasons for the differences between model simulations and observations. Factors such as measurement uncertainties (due to sample treatment and analysis methodology), temporal (inter-annual and seasonal) and spatial variations of BC deposition, and vertical variations of BC in snowpack, can strongly affect the accuracy and representativeness of BC-in-snow measurements for the purpose of evaluating global models. Ming et al. (2013) and Qian et al. (2015) pointed out that BC concentrations in snow and ice samples over HTP tend to decrease with increasing glacier elevations, while global models with coarse grid resolution cannot accurately represent elevation of sampling sites. Often times the difference is significant. Nonetheless, it is likely that positive biases exist in the modeled concentration and radiative forcing of BC and dust in snow.

Black carbon over the Himalayas and Tibetan Plateau

R. Zhang et al.

Title Page

Abstract

Introduction

Conclusions

References

Tables

Figures



Back

Close

Full Screen / Esc

Printer-friendly Version

Interactive Discussion



6 Summary and conclusions

In this study, we employed the CAM5 model with a newly developed source tagging technique, nudged towards the MERRA meteorological reanalysis, to characterize the fate of BC particles emitted from various geographical regions and sectors to the HTP region. In addition, we compare the radiative forcing induced by BC in the atmosphere and in snow over the HTP, as well as forcing induced by dust in snow. Although there are biases in the simulated BC, partly due to the inherent difficulty for coarse-resolution global models to accurately represent transport and wet deposition in this topographically complex region, the CAM5 model simulation shows a reasonable agreement in the seasonal variation of the near-surface airborne BC concentrations with observations over the HTP and surrounding regions. This provides us the confidence to use this modeling framework to characterize BC source–receptor relationships in the HTP.

The explicit source tagging technique enables the characterization of three-dimensional transport pathways of BC to the HTP from different geographical regions and source sectors, which also depends on seasons and the location of the receptor in the HTP. With the IPCC AR5 present-day emission inventories, the annual mean BC column burden and surface deposition in the entire HTP region is contributed the most by biomass and biofuel (BB) emissions from South Asia (SAS) (33 and 40 %, respectively), followed by fossil fuel (FF) emissions from SAS (17 and 20 %, respectively), and then the FF from East Asia (EAS) (14 and 14 %, respectively). The same roles hold for all the seasonal means except for the summer when the EAS FF becomes more important. Although BC emissions from the entire EAS source region are much stronger than those from SAS, the concentrated FF BC emissions in central-eastern China are only transported towards the HTP during the East Asian summer monsoon. Thus seasonal prevailing winds are important in determining the seasonal variations in BC transport and source–receptor relationships.

For the multiple finer receptor regions of interest, SAS BB and FF have the largest impact on BC in Himalayas and Central Plateau, while EAS FF and BB contribute the

ACPD

15, 77–121, 2015

Black carbon over the Himalayas and Tibetan Plateau

R. Zhang et al.

Title Page

Abstract

Introduction

Conclusions

References

Tables

Figures



Back

Close

Full Screen / Esc

Printer-friendly Version

Interactive Discussion



most to Northeast Plateau in all seasons and Southeast Plateau in the summer. The Central Asia (CAS) and Middle East (MDE) FF emissions make important contributions to BC over the Northwest Plateau, especially from CAS in JJA.

The HTP BC is most sensitive by far to per unit changes in the local emissions, although they only contribute about 10 % of the BC burden in the HTP. The SAS region makes large contributions to BC burden and deposition over the HTP and the BC sensitivities to SAS emissions are also high for almost all of the sub-regions of HTP, especially the Himalayas. BC over the Northeast Plateau is quite sensitive to EAS emissions in all seasons, and Southeast Plateau BC is also sensitive to EAS emissions in JJA. Although BC emissions from MDE and CAS are weak and their contribution to the HTP overall is low, their efficiencies are quite high. BC over Northwest Plateau and Central Plateau is extremely sensitive to emissions from CAS in JJA. These source–receptor relationships and sensitivities can be useful to policymakers for improving the effective mitigation road map in order to potentially slow down the glacier retreat in the HTP region.

The impact of BC on snow and glacier melting can be characterized by the magnitude of radiative forcing. Our calculations show that the annual mean BC-in-snow radiative forcing (0.42 W m^{-2}) outweighs BC dimming effect (-0.3 W m^{-2}) at the surface over the HTP. In the five sub-regions, the annual mean BC-in-snow forcing ranges from 0.04 W m^{-2} in the Central Plateau to 1.75 W m^{-2} in the Northwest Plateau. We also showed that the annual mean dust-in-snow induced radiative forcing over the HTP can be quite significant (0.33 W m^{-2} for entire the HTP, and 0.99 W m^{-2} for the Northwest Plateau). More importantly, both BC- and dust-in-snow forcing peaks in the spring melting season when the area-average forcing reaches 1.03 and 0.87 W m^{-2} , respectively, over the entire HTP, and their combined forcing is more than 8 W m^{-2} over the Northwest Plateau. Such a large forcing is sufficient to cause earlier snow melting and contribute to the acceleration of glacier retreat, although the model is likely to overestimate BC-in-snow forcing due to the possible positive bias of snow cover fraction in the winter and early spring. According to our estimates of the source attribution, the

Black carbon over the Himalayas and Tibetan Plateau

R. Zhang et al.

Title Page

Abstract

Introduction

Conclusions

References

Tables

Figures



Back

Close

Full Screen / Esc

Printer-friendly Version

Interactive Discussion



Black carbon over the Himalayas and Tibetan Plateau

R. Zhang et al.

Title Page

Abstract

Introduction

Conclusions

References

Tables

Figures



Back

Close

Full Screen / Esc

Printer-friendly Version

Interactive Discussion



biomass burning and biofuel emissions in South Asia contribute the most to annual mean forcing over the HTP and its sub-regions except for the Northeast Plateau where the largest contribution is from East Asia fossil fuel emissions. During the winter and spring seasons over Northwest Plateau and Himalayas, when and where the forcing is the largest, South Asia (especially the biomass burning and biofuel sector) is the major contributor.

The Supplement related to this article is available online at doi:10.5194/acpd-15-77-2015-supplement.

Acknowledgements. This research is based on work supported by the U.S. Department of Energy (DOE), Office of Science, Biological and Environmental Research as part of the Earth System Modeling Program. The Pacific Northwest National Laboratory (PNNL) is operated for DOE by Battelle Memorial Institute under contract DE-AC05-76RLO1830. The CESM project is supported by the National Science Foundation and the DOE Office of Science. R. Zhang acknowledges support from the China Scholarship Fund. J. Huang and Q. Fu acknowledge support from the National Basic Research Program of China (2012CB955303), NSFC grant 41275070 and China 111 project (No. B13045). Computational resources were provided by the National Energy Research Scientific Computing Center (NERSC), a national scientific user facility located at Lawrence Berkeley National Laboratory in Berkeley, California. NERSC is the flagship scientific computing facility for the Office of Science in DOE.

References

Babu, S. S., Chaubey, J. P., Moorthy, K. K., Gogoi, M. M., Kompalli, S. K., Sreekanth, V., Bagare, S. P., Bhatt, B. C., Gaur, V. K., Prabhu, T. P., and Singh, N. S.: High altitude (~4520 m amsl) measurements of black carbon aerosols over western trans-Himalayas: seasonal heterogeneity and source apportionment, *J. Geophys. Res.*, 116, D24201, doi:10.1029/2011JD016722, 2011.

Black carbon over the Himalayas and Tibetan Plateau

R. Zhang et al.

Title Page

Abstract

Introduction

Conclusions

References

Tables

Figures



Back

Close

Full Screen / Esc

Printer-friendly Version

Interactive Discussion



Barnett, T. P., Adam, J. C., and Lettenmaier, D. P.: Potential impacts of a warming climate on water availability in snow-dominated regions, *Nature*, 438, 303–309, doi:10.1038/Nature04141, 2005.

Bolch, T., Kulkarni, A., Kääb, A., Huggel, C., Paul, F., Cogley, J., Frey, H., Kargel, J., Fujita, K., Scheel, M., Bajracharya, S., and Stoffel, M.: The state and fate of Himalayan Glaciers, *Science*, 336, 310–314, doi:10.1126/science.1215828, 2012.

Bond, T. C., Bhardwaj, E., Dong, R., Jogani, R., Jung, S., Roden, C., Streets, D. G., and Trautmann, N. M.: Historical emissions of black and organic carbon aerosol from energy-related combustion, 1850–2000, *Global Biogeochem. Cy.*, 21, GB2018, doi:10.1029/2006GB002840, 2007.

Bond, T. C., Doherty, S. J., Fahey, D. W., Forster, P. M., Berntsen, T., DeAngelo, B. J., Flanner, M. G., Ghan, S., Kärcher, B., Koch, D., Kinne, S., Kondo, Y., Quinn, P. K., Sarofim, M. C., Schultz, M. G., Schulz, M., Venkataraman, C., Zhang, H., Zhang, S., Bellouin, N., Gutikunda, S. K., Hopke, P. K., Jacobson, M. Z., Kaiser, J. W., Klimont, Z., Lohmann, U., Schwarz, J. P., Shindell, D., Storelvmo, T., Warren, S. G., and Zender, C. S.: Bounding the role of black carbon in the climate system: a scientific assessment, *J. Geophys. Res.-Atmos.*, 118, 5380–5552, doi:10.1002/jgrd.50171, 2013.

Bonasoni, P., Laj, P., Marinoni, A., Sprenger, M., Angelini, F., Arduini, J., Bonafè, U., Calzolari, F., Colombo, T., Decesari, S., Di Biagio, C., di Sarra, A. G., Evangelisti, F., Duchi, R., Facchini, MC., Fuzzi, S., Gobbi, G. P., Maione, M., Panday, A., Roccatò, F., Sellegri, K., Venzac, H., Verza, GP., Villani, P., Vuillermoz, E., and Cristofanelli, P.: Atmospheric Brown Clouds in the Himalayas: first two years of continuous observations at the Nepal Climate Observatory-Pyramid (5079 m), *Atmos. Chem. Phys.*, 10, 7515–7531, doi:10.5194/acp-10-7515-2010, 2010.

Cao, J. J., Xu, B. Q., He, J. Q., Liu, X. Q., Han, Y. M., Wang, G. H., and Zhu, C. S.: Concentrations, seasonal variations, and transport of carbonaceous aerosol at a remote Mountainous region in western China, *Atmos. Environ.*, 43, 4444–4452, doi:10.1016/j.atmosenv.2009.06.023, 2009.

Chen, S., Huang, J., Zhao, C., Qian, Y., Leung, L. R., and Yang, B.: Modeling the transport and radiative forcing of Taklimakan dust over the Tibetan Plateau in summer, *J. Geophys. Res.*, 118, 797–812, doi:10.1002/jgrd.50122, 2013.

Conway, H., Gades, A., and Raymond, C. F.: Albedo of dirty snow during conditions of melt, *Water Resour. Res.*, 32, 1713–1718, doi:10.1029/96WR00712, 1996.

Black carbon over the Himalayas and Tibetan Plateau

R. Zhang et al.

Title Page

Abstract

Introduction

Conclusions

References

Tables

Figures



Back

Close

Full Screen / Esc

Printer-friendly Version

Interactive Discussion



- Dentener, F., Kinne, S., Bond, T., Boucher, O., Cofala, J., Generoso, S., Ginoux, P., Gong, S., Hoelzemann, J. J., Ito, A., Marelli, L., Penner, J. E., Putaud, J.-P., Textor, C., Schulz, M., van der Werf, G. R., and Wilson, J.: Emissions of primary aerosol and precursor gases in the years 2000 and 1750 prescribed data-sets for AeroCom, *Atmos. Chem. Phys.*, 6, 4321–4344, doi:10.5194/acp-6-4321-2006, 2006.
- Doherty, S. J., Dang, C., Hegg, D. A., Zhang, R., and Warren, S. G.: Black carbon and other light-absorbing particles in snow of central North America, *J. Geophys. Res. Atmos.*, 119, 12807–12831, doi:10.1002/2014JD022350, 2014.
- Duan, A., Wu, G., Zhang, Q., and Liu, Y.: New proofs of the recent climate warming over the Tibetan Plateau as a result of the increasing greenhouse gases emissions, *Chinese Sci. Bull.*, 51, 1396–1400, doi:10.1007/s11434-006-1396-6, 2006.
- Duan, A. M. and Wu, G. X.: Weakening trend in the atmospheric heat source over the Tibetan Plateau during recent decades. Part I: Observations, *J. Climate*, 21, 3149–3164, doi:10.1175/2007JCLI1912.1, 2008.
- Flanner, M. G., Zender, C. S., Randerson, J. T., and Rasch, P. J.: Present day climate forcing and response from black carbon in snow, *J. Geophys. Res.*, 112, D11202, doi:10.1029/2006JD008003, 2007.
- Flanner, M. G., Zender, C. S., Hess, P. G., Mahowald, N. M., Painter, T. H., Ramanathan, V., and Rasch, P. J.: Springtime warming and reduced snow cover from carbonaceous particles, *Atmos. Chem. Phys.*, 9, 2481–2497, doi:10.5194/acp-9-2481-2009, 2009.
- Gettelman, A., Liu, X., Ghan, S. J., Morrison, H., Park, S., Conley, A. J., Klein, S. A., Boyle, J., Mitchell, D. L., and Li, J. L. F.: Global simulations of ice nucleation and ice supersaturation with an improved cloud scheme in the Community Atmosphere Model, *J. Geophys. Res.*, 115, D18216, doi:10.1029/2009jd013797, 2010.
- Ginot, P., Dumont, M., Lim, S., Patris, N., Taupin, J.-D., Wagnon, P., Gilbert, A., Arnaud, Y., Marinoni, A., Bonasoni, P., and Laj, P.: A 10 year record of black carbon and dust from a Mera Peak ice core (Nepal): variability and potential impact on melting of Himalayan glaciers, *The Cryosphere*, 8, 1479–1496, doi:10.5194/tc-8-1479-2014, 2014.
- Hadley, O. L. and Kirchstetter, T. W.: Black-carbon reduction of snow albedo, *Nat. Clim. Change*, 2, 437–440, 2012.
- Hall, A. and Qu, X.: Using the current seasonal cycle to constrain snow albedo feedback in future climate change, *Geophys. Res. Lett.*, 33, L03502, doi:10.1029/2005GL025127, 2006.

Black carbon over the Himalayas and Tibetan Plateau

R. Zhang et al.

Title Page

Abstract

Introduction

Conclusions

References

Tables

Figures



Back

Close

Full Screen / Esc

Printer-friendly Version

Interactive Discussion



Hall, D. K., Riggs, G. A., and Salomonson, V. V.: MODIS/TERRA Snow Cover Monthly L3 Global 0.05Deg CMG V005, [2001], Boulder, CO, National Snow and Ice Data Center. Digital Media, distributed in netCDF format by the Integrated Climate Data Center (ICDC, available at: <http://icdc.zmaw.de> (last access: 26 December 2014) University of Hamburg, Hamburg, Germany), updated monthly, 2006.

Hansen, J. and Nazarenko, L.: Soot climate forcing via snow and ice albedos, *P. Natl. Acad. Sci. USA*, 101, 423–428, doi:10.1073/pnas.2237157100, 2004.

Hansen, J., Sato, M., Ruedy, R., Nazarenko, L., Lacis, A., Schmidt, G. A., Russell, G., Aleinov, I., Bauer, M., Bauer, S., Bell, N., Cairns, B., Canuto, V., Chandler, M., Cheng, Y., Del Genio, A., Faluvegi, G., Fleming, E., Friend, A., Hall, T., Jackman, C., Kelley, M., Kiang, N., Koch, D., Lean, J., Lerner, J., Lo, K., Menon, S., Miller, R., Minnis, P., Novakov, T., Oinas, V., Perlwitz, J., Perlwitz, Ju., Rind, D., Romanou, A., Shindell, D., Stone, P., Sun, S., Tausnev, N., Thresher, D., Wielicki, B., Wong, T., Yao, M., and Zhang, S.: Efficacy of climate forcings, *J. Geophys. Res.*, 110, D18104, doi:10.1029/2005JD005776, 2005.

Huang, J., Minnis, P., Yi, Y., Tang, Q., Wang, X., Hu, Y., Liu, Z., Ayers, K., Trepte, C., and Winker, D.: Summer dust aerosols detected from CALIPSO over the Tibetan Plateau, *Geophys. Res. Lett.*, 34, L18805, doi:10.1029/2007GL029938, 2007.

Huang, J., Fu, Q., Zhang, W., Wang, X., Zhang, R., Ye, H., and Warren, S. G.: Dust and black carbon in seasonal snow across Northern China, *B. Am. Meteorol. Soc.*, 92, 175–181, doi:10.1175/2010BAMS3064.1, 2011.

Hurrell, J. W., Holland, M. M., Ghan, S., Lamarque, J.-F., Lawrence, D., Lipscomb, W. H., Mahowald, N., Marsh, D., Rasch, P., Bader, D., Collins, W. D., Gent, P. R., Hack, J. J., Kiehl, J., Kushner, P., Large, W. G., Marshall, S., Vavrus, S., and Vertenstein, M.: The Community Earth System Model: a framework for collaborative research, *B. Am. Meteorol. Soc.*, 94, 1339–1360, doi:10.1175/BAMS-D-12-00121, 2013.

Immerzeel, W., VanBeek, L. P. H., and Bierkens, M. F. P.: Climate change will affect the Asian water towers, *Science*, 328, 1382–1385, doi:10.1126/science.1183188, 2010.

IPCC: Summary for policymakers, in: *Climate Change 2013: The Physical Science Basis. Contribution of Working Group I to the Fifth Assessment Report of the Intergovernmental Panel on Climate Change*, edited by: Stocker, T. F., Qin, D., Plattner, G.-K., Tignor, M., Allen, S. K., Boschung, J., Nauels, A., Xia, Y., Bex, V., and Midgley, P. M., Cambridge University Press, Cambridge, UK, New York, NY, USA, 2013.

Black carbon over the Himalayas and Tibetan Plateau

R. Zhang et al.

Title Page

Abstract

Introduction

Conclusions

References

Tables

Figures



Back

Close

Full Screen / Esc

Printer-friendly Version

Interactive Discussion



Jacobson, M. Z.: Climate response of fossil fuel and biofuel soot, accounting for soot's feedback to snow and sea ice albedo and emissivity, *J. Geophys. Res.*, 109, D21201, doi:10.1029/2004JD004945, 2004.

Jiao, C., Flanner, M. G., Balkanski, Y., Bauer, S. E., Bellouin, N., Berntsen, T. K., Bian, H., Carslaw, K. S., Chin, M., De Luca, N., Diehl, T., Ghan, S. J., Iversen, T., Kirkevåg, A., Koch, D., Liu, X., Mann, G. W., Penner, J. E., Pitari, G., Schulz, M., Seland, Ø., Skeie, R. B., Steenrod, S. D., Stier, P., Takemura, T., Tsigaridis, K., van Noije, T., Yun, Y., and Zhang, K.: An AeroCom assessment of black carbon in Arctic snow and sea ice, *Atmos. Chem. Phys.*, 14, 2399–2417, doi:10.5194/acp-14-2399-2014, 2014.

Kang, S., Wake, C., Qin, D., Mayewski, P. A., and Yao, T.: Monsoon and dust signals recorded in Dasuopu glacier, Tibetan Plateau, *J. Glaciol.*, 46, 222–226, 2000.

Kang, S., Wei, X., You, Q., Flugel, W., Pepin, N., and Yao, T.: Review of climate and cryospheric change in the Tibetan Plateau, *Environ. Res. Lett.*, 5, 015101, doi:10.1088/1748-9326/5/1/015101, 2010.

Kaser, G., Grosshauser, M., and Marzeion, B.: Contribution of glaciers to water availability in different climate regimes, *P. Natl. Acad. Sci. USA*, 107, 20223–20227, doi:10.1073/pnas.1008162107, 2010

Kaspari, S. D., Schwikowski, M., Gysel, M., Flanner, M. G., Kang, S., Hou, S., and Mayewski, P. A.: Resent increase in black carbon concentrations from a Mt. Everest ice core spanning 1860–2000 AD, *Geophys. Res. Lett.*, 38, L04703, doi:10.1029/2010GL046096, 2011.

Kopacz, M., Mauzerall, D. L., Wang, J., Leibensperger, E. M., Henze, D. K., and Singh, K.: Origin and radiative forcing of black carbon transported to the Himalayas and Tibetan Plateau, *Atmos. Chem. Phys.*, 11, 2837–2852, doi:10.5194/acp-11-2837-2011, 2011.

Lamarque, J.-F., Bond, T. C., Eyring, V., Granier, C., Heil, A., Klimont, Z., Lee, D., Liousse, C., Mieville, A., Owen, B., Schultz, M. G., Shindell, D., Smith, S. J., Stehfest, E., Van Aardenne, J., Cooper, O. R., Kainuma, M., Mahowald, N., McConnell, J. R., Naik, V., Riahi, K., and van Vuuren, D. P.: Historical (1850–2000) gridded anthropogenic and biomass burning emissions of reactive gases and aerosols: methodology and application, *Atmos. Chem. Phys.*, 10, 7017–7039, doi:10.5194/acp-10-7017-2010, 2010.

Lamarque, J.-F., Emmons, L. K., Hess, P. G., Kinnison, D. E., Tilmes, S., Vitt, F., Heald, C. L., Holland, E. A., Lauritzen, P. H., Neu, J., Orlando, J. J., Rasch, P. J., and Tyndall, G. K.: CAM-

Black carbon over the Himalayas and Tibetan Plateau

R. Zhang et al.

Title Page

Abstract

Introduction

Conclusions

References

Tables

Figures



Back

Close

Full Screen / Esc

Printer-friendly Version

Interactive Discussion



- chem: description and evaluation of interactive atmospheric chemistry in the Community Earth System Model, *Geosci. Model Dev.*, 5, 369–411, doi:10.5194/gmd-5-369-2012, 2012.
- Lau, K. M., Kim, M. K., and Kim, K. M.: Asian monsoon anomalies induced by aerosol direct forcing: the role of the Tibetan Plateau, *Clim. Dynam.*, 26, 855–664, 2006.
- 5 Lau, K.-M., Kim, M. K., Kim, K.-M., and Lee, W. S.: Enhanced surface warming and accelerated snow melt in the Himalayas and Tibetan Plateau induced by absorbing aerosols, *Environ. Res. Lett.*, 5, 025204, doi:10.1088/1748-9326/5/2/025204, 2010.
- Lee, Y. H., Lamarque, J.-F., Flanner, M. G., Jiao, C., Shindell, D. T., Berntsen, T., Bisiaux, M. M., Cao, J., Collins, W. J., Curran, M., Edwards, R., Faluvegi, G., Ghan, S., Horowitz, L. W., Mc-
 10 Connell, J. R., Ming, J., Myhre, G., Nagashima, T., Naik, V., Rumbold, S. T., Skeie, R. B., Sudo, K., Takemura, T., Thevenon, F., Xu, B., and Yoon, J.-H.: Evaluation of preindustrial to present-day black carbon and its albedo forcing from Atmospheric Chemistry and Climate Model Intercomparison Project (ACCMIP), *Atmos. Chem. Phys.*, 13, 2607–2634, doi:10.5194/acp-13-2607-2013, 2013.
- 15 Li, X., Cheng, G., Jin, H., Kang, E., Che, T., Jin, R., Wu, L., Nan, Z., Wang, J., and Shen, Y.: Cryospheric change in China, *Global Planet. Change*, 62, 210–218, 2008.
- Liu, X., Easter, R. C., Ghan, S. J., Zaveri, R., Rasch, P., Shi, X., Lamarque, J.-F., Gettelman, A., Morrison, H., Vitt, F., Conley, A., Park, S., Neale, R., Hannay, C., Ekman, A. M. L., Hess, P., Mahowald, N., Collins, W., Iacono, M. J., Bretherton, C. S., Flanner, M. G., and
 20 Mitchell, D.: Toward a minimal representation of aerosols in climate models: description and evaluation in the Community Atmosphere Model CAM5, *Geosci. Model Dev.*, 5, 709–739, doi:10.5194/gmd-5-709-2012, 2012.
- Liu, Z., Liu, D., Huang, J., Vaughan, M., Uno, I., Sugimoto, N., Kittaka, C., Trepte, C., Wang, Z., Hostetler, C., and Winker, D.: Airborne dust distributions over the Tibetan Plateau and surrounding areas derived from the first year of CALIPSO lidar observations, *Atmos. Chem. Phys.*, 8, 5045–5060, doi:10.5194/acp-8-5045-2008, 2008.
- 25 Lu, Z., Streets, D. G., Zhang, Q., and Wang, S.: A novel back-trajectory analysis of the origin of black carbon transported to the Himalayas and Tibetan Plateau during 1996–2010, *Geophys. Res. Lett.*, 39, L01809, doi:10.1029/2011GL049903, 2012.
- 30 Ma, P.-L., Rasch, P. J., Wang, H., Zhang, K., Easter, R. C., Tilmes, S., Fast, J. D., Liu, X., Yoon, J.-H., and Lamarque, J.-F.: The role of circulation features on black carbon transport into the Arctic in the Community Atmosphere Model Version 5 (CAM5), *J. Geophys. Res.-Atmos.*, 118, 4657–4669, 2013.

Black carbon over the Himalayas and Tibetan Plateau

R. Zhang et al.

Title Page

Abstract

Introduction

Conclusions

References

Tables

Figures



Back

Close

Full Screen / Esc

Printer-friendly Version

Interactive Discussion



- Manabe, S. and Terpstra, T. B.: The effects of mountains on the general circulation of the atmosphere as identified by numerical experiments, *J. Atmos. Sci.*, 31, 3–42, 1974.
- Marinoni, A., Cristofanelli, P., Laj, P., Duchi, R., Calzolari, F., Decesari, S., Sellegri, K., Vuillermoz, E., Verza, G. P., Villani, P., and Bonasoni, P.: Aerosol mass and black carbon concentrations, a two year record at NCO-P (5079 m, Southern Himalayas), *Atmos. Chem. Phys.*, 10, 8551–8562, doi:10.5194/acp-10-8551-2010, 2010.
- Marinoni, A., Cristofanelli, P., Laj, P., Duchi, R., Putero, D., Calzolari, F., Landi, T. C., Vuillermoz, E., Maione, M., and Bonasoni, P.: High black carbon and ozone concentrations during pollution transport in the Himalayas: five years of continuous observations at NCO-P global GAW station, *J. Environ. Sci.*, 25, 1618–1625, doi:10.1016/S1001-0742(12)60242-3, 2013.
- Ménégoz, M., Krinner, G., Balkanski, Y., Boucher, O., Cozic, A., Lim, S., Ginot, P., Laj, P., Gallée, H., Wagnon, P., Marinoni, A., and Jacobi, H. W.: Snow cover sensitivity to black carbon deposition in the Himalayas: from atmospheric and ice core measurements to regional climate simulations, *Atmos. Chem. Phys.*, 14, 4237–4249, doi:10.5194/acp-14-4237-2014, 2014.
- Menon, S., Hansen, J., Nazarenko, L., and Luo, Y.: Climate effects of black carbon aerosols in China and India, *Science*, 297, 2250–2253, doi:10.1126/science.1075159, 2002.
- Menon, S., Koch, D., Beig, G., Sahu, S., Fasullo, J., and Orlikowski, D.: Black carbon aerosols and the third polar ice cap, *Atmos. Chem. Phys.*, 10, 4559–4571, doi:10.5194/acp-10-4559-2010, 2010.
- Ming, J., Cachier, H., Xiao, C., Qin, D., Kang, S., Hou, S., and Xu, J.: Black carbon record based on a shallow Himalayan ice core and its climatic implications, *Atmos. Chem. Phys.*, 8, 1343–1352, doi:10.5194/acp-8-1343-2008, 2008.
- Ming, J., Xiao, C. D., Cachier, H., Qin, D. H., Qin, X., Li, Z. Q., and Pu, J. C.: Black carbon (bc) in the snow of glaciers in west china and its potential effects on albedos, *Atmos. Res.*, 92, 114–123, doi:10.1016/j.atmosres.2008.09.007, 2009.
- Ming, J., Xiao, C., Sun, J., Kang, S., and Bonasoni, P.: Carbonaceous particles in the atmosphere and precipitation of the Nam Co region, central Tibet, *J. Environ. Sci.*, 22, 1748–1756, doi:10.1016/S1001-0742(09)60315-6, 2010.
- Ming, J., Xiao, C., Du, Z., and Yang, X.: An overview of black carbon deposition in High Asia glaciers and its impacts on radiation balance, *Adv. Water Resour.*, 55, 80–87, 2013.

Black carbon over the Himalayas and Tibetan Plateau

R. Zhang et al.

Title Page

Abstract

Introduction

Conclusions

References

Tables

Figures



Back

Close

Full Screen / Esc

Printer-friendly Version

Interactive Discussion



- Moorthy, K. K., Beegum, S. N., Srivastava, N., Satheesh, S. K., Chin, M., Blond, N., Babu, S. S., and Singh, S.: Performance evaluation of chemistry transport models over India, *Atmos. Environ.*, 71, 210–225, 2013.
- Neale, R. B., Chen, C.-C., Gettelman, A., Lauritzen, P. H., Park, S., Williamson, D. L., Conley, A. J., Garcia, R., Kinnison, D., Lamarque, J.-F., Marsh, D., Mills, M., Smith, A. K., Tilmes, S., Vitt, F., Cameron-Smith, P., Collins, W. D., Iacono, M. J., Easter, R. C., Ghan, S. J., Liu, X., Rasch, P. J., and Taylor, M. A.: Description of the NCAR Community Atmosphere Model (CAM 5.0), NCAR/TN-486+STR, available at: http://www.cesm.ucar.edu/models/cesm1.0/cam/docs/description/cam5_desc.pdf (last access: 26 December 2014), 2012.
- Ohara, T., Akimoto, H., Kurokawa, J., Horii, N., Yamaji, K., Yan, X., and Hayasaka, T.: An Asian emission inventory of anthropogenic emission sources for the period 1980–2020, *Atmos. Chem. Phys.*, 7, 4419–4444, doi:10.5194/acp-7-4419-2007, 2007.
- Petzold, A., Ogren, J. A., Fiebig, M., Laj, P., Li, S.-M., Baltensperger, U., Holzer-Popp, T., Kinne, S., Pappalardo, G., Sugimoto, N., Wehrl, C., Wiedensohler, A., and Zhang, X.-Y.: Recommendations for reporting “black carbon” measurements, *Atmos. Chem. Phys.*, 13, 8365–8379, doi:10.5194/acp-13-8365-2013, 2013.
- Prasad, A. K. and Singh, R. P.: Changes in Himalayan snow and glacier cover between 1972 and 2000, *Eos T. Am. Geophys. Un.*, 88, 33, doi:10.1029/2007EO330002, 2007.
- Pu, Z., Xu, L., and Salomonson, V. V.: MODIS/Terra observed seasonal variations of snow cover over the Tibetan Plateau, *Geophys. Res. Lett.*, 34, L06706, doi:10.1029/2007GL029262, 2007.
- Qian, Y., Flanner, M. G., Leung, L. R., and Wang, W.: Sensitivity studies on the impacts of Tibetan Plateau snowpack pollution on the Asian hydrological cycle and monsoon climate, *Atmos. Chem. Phys.*, 11, 1929–1948, doi:10.5194/acp-11-1929-2011, 2011.
- Qian, Y., Wang, H., Zhang, R., Flanner, M. G., and Rasch, P. J.: A sensitivity study on modeling black carbon in snow and its radiative forcing over the Arctic and Northern China, *Environ. Res. Lett.*, 9, 064001, doi:10.1088/1748-9326/9/6/064001, 2014.
- Qian, Y., Yasunari, T. J., Doherty, S. J., Flanner, M. G., Lau, K. M., Ming, J., Wang, H., Wang, M., Warren, S. G., and Zhang, R.: Light-absorbing particles in snow and ice: measurement and modeling of climatic and hydrological impact, *Adv. Atmos. Sci.*, 32, 64–91, doi:10.1007/s00376-014-0010-0, 2015.
- Qin, D., Liu, S., and Li, P.: Snow cover distribution, variability, and response to climate change in western China, *J. Climate*, 19, 1820–1833, 2006.

**Black carbon over
the Himalayas and
Tibetan Plateau**

R. Zhang et al.

[Title Page](#)[Abstract](#)[Introduction](#)[Conclusions](#)[References](#)[Tables](#)[Figures](#)[Back](#)[Close](#)[Full Screen / Esc](#)[Printer-friendly Version](#)[Interactive Discussion](#)

Qiu, J.: China: the third pole, *Nature News*, 454, 393–396, 2008.

Ram, K., Sarin, M. M., and Hegde, P.: Long-term record of aerosol optical properties and chemical composition from a high-altitude site (Manora Peak) in Central Himalaya, *Atmos. Chem. Phys.*, 10, 11791–11803, doi:10.5194/acp-10-11791-2010, 2010.

5 Ramanathan, V., Ramana, M. V., Roberts, G., Kim, D., Corrigan, C., Chung, C., and Winker, D.: Warming trends in Asia amplified by brown clouds solar absorption, *Nature*, 448, 575–578, 2007.

Rasch, P. J., Mahowald, N. M., and Eaton, B. E.: Representations of transport, convection, and the hydrological cycle in chemical transport models: implications for the modeling of short-lived and soluble species, *J. Geophys. Res.*, 102, 28127–28138, 1997.

10 Ren, J., Jing, Z., Pu, J., and Qin, X.: Glaciers variations and climate change in the central Himalaya over the past few decades, *Ann. Glaciol.*, 43, 218–222, 2006.

Rienecker, M. M., Suarez, M. J., Gelaro, R., Todling, R., Bacmeister, J., Liu, E., Bosilovich, M. G., Schubert, S. D., Takacs, L., Kim, G.-K., Bloom, S., Chen, J., Collins, D., Conaty, A., da Silva, A., Gu, W., Joiner, J., Koster, R. D., Lucchesi, R., and Molod, A.: MERRA – NASA’s Modern-Era Retrospective Analysis for Research and Applications, *J. Climate*, 24, 3624–3648, 2011.

Singh, P. and Bengtsson, L.: Hydrological sensitivity of a large Himalayan basin to climate change, *Hydrol. Process.*, 18, 2363–2385, 2004.

20 Taylor, K. E., Stouffer, R. J., and Meehl, G. A.: An overview of CMIP5 and the experiment design, *B. Am. Meteorol. Soc.*, 93, 485–498, doi:10.1175/BAMS-D-11-00094.1, 2012.

Wang, B., Bao, Q., Hoskins, B., Wu, G., and Liu, Y.: Tibetan Plateau warming and precipitation changes in East Asia, *Geophys. Res. Lett.*, 35, L14702, doi:10.1029/2008GL034330, 2008.

25 Wang, H., Easter, R. C., Rasch, P. J., Wang, M., Liu, X., Ghan, S. J., Qian, Y., Yoon, J.-H., Ma, P.-L., and Vinoj, V.: Sensitivity of remote aerosol distributions to representation of cloud–aerosol interactions in a global climate model, *Geosci. Model Dev.*, 6, 765–782, doi:10.5194/gmd-6-765-2013, 2013.

Wang, H., Rasch, P. J., Easter, R. C., Singh, B., Zhang, R., Ma, P. L., Qian, Y., and Beagley, N.: Using an explicit emission tagging method in global modeling of source–receptor relationships for black carbon in the Arctic: variations, sources and transport pathways, *J. Geophys. Res.-Atmos.*, 119, 12888–12909, doi:10.1002/2014JD022297, 2014.

30 Wang, M., Xu, B., Cao, J., Tie, X., Wang, H., Zhang, R., Qian, Y., Rasch, P. J., Zhao, S., Wu, G., Zhao, H., Joswiak, D. R., Li, J., and Xie, Y.: Carbonaceous aerosols recorded in a

Black carbon over the Himalayas and Tibetan Plateau

R. Zhang et al.

Title Page

Abstract

Introduction

Conclusions

References

Tables

Figures



Back

Close

Full Screen / Esc

Printer-friendly Version

Interactive Discussion



Southeastern Tibetan glacier: variations, sources and radiative forcing, *Atmos. Chem. Phys. Discuss.*, 14, 19719–19746, doi:10.5194/acpd-14-19719-2014, 2014.

Wang, X., Doherty, S. J., and Huang, J.: Black carbon and other light-absorbing impurities in snow across Northern China, *J. Geophys. Res.-Atmos.*, 118, 1471–1492, doi:10.1029/2012JD018291, 2013.

Warren, S. G. and Wiscombe, W. J.: A model for the spectral albedo of snow. II: Snow containing atmospheric aerosols, *J. Atmos. Sci.*, 37, 2734–2745, 1980.

Warren, S. G. and Wiscombe, W. J.: Dirty snow after nuclear war, *Nature*, 313, 469–470, 1985.

Wu, G., Liu, Y., He, B., Bao, Q., Duan, A., and Jin, F.-F.: Thermal controls on the Asian summer monsoon, *Sci. Rep.*, 2, 404, doi:10.1038/srep00404, 2012.

Xia, X. G., Zong, X. M., Cong, Z. Y., Chen, H. B., Kang, S. C., and Wang, P. C.: Baseline continental aerosol over the central Tibetan plateau and a case study of aerosol transport from South Asia, *Atmos. Environ.*, 45, 7370–7378, 2011.

Xu, B., Cao, J., Hansen, J., Yao, T., Joswiak, D. R., Wang, N., Wu, G., Wang, M., Zhao, H., Yang, W., Liu, X., and He, J.: Black soot and the survival of Tibetan glaciers, *P. Natl. Acad. Sci. USA*, 106, 22114–22118, 2009.

Xu, X., Lu, C., Shi, X., and Gao, S.: World water tower: an atmospheric perspective, *Geophys. Res. Lett.*, 35, L20815, doi:10.1029/2008GL035867, 2008.

Yanai, M., Li, C., and Song, Z.: Seasonal heating of the Tibetan Plateau and its effects on the evolution of the Asian summer monsoon, *J. Meteorol. Soc. Jpn.*, 70, 319–351, 1992.

Yao, T., Pu, J., Lu, A., Wang, Y., and Yu, W.: Recent glacial retreat and its impact on hydrological processes on the Tibetan Plateau, China, and surrounding regions, *Arct. Antarct. Alp. Res.*, 39, 642–650, 2007.

Yao, T., Thompson, L., Yang, W., Yu, W., Gao, Y., Guo, X., Yang, X., Duan, K., Zhao, H., Xu, B., Pu, J., Lu, A., Xiang, Y., Kattel, D. B., and Joswiak, D.: Different glacier status with atmospheric circulations in Tibetan Plateau and surroundings, *Nat. Clim. Change*, 2, 663–667, doi:10.1038/nclimate1580, 2012.

Yasunari, T. J., Bonasoni, P., Laj, P., Fujita, K., Vuillermoz, E., Marinoni, A., Cristofanelli, P., Duchi, R., Tartari, G., and Lau, K.-M.: Estimated impact of black carbon deposition during pre-monsoon season from Nepal Climate Observatory – Pyramid data and snow albedo changes over Himalayan glaciers, *Atmos. Chem. Phys.*, 10, 6603–6615, doi:10.5194/acp-10-6603-2010, 2010.

Black carbon over the Himalayas and Tibetan Plateau

R. Zhang et al.

Title Page

Abstract

Introduction

Conclusions

References

Tables

Figures



Back

Close

Full Screen / Esc

Printer-friendly Version

Interactive Discussion



- Ye, D. and Gao, Y.: Meteorology of the Qinghai-Xizang Plateau, Chinese Science Press, Beijing, 1979.
- Ye, D. and Wu, G.: The role of the heat source of the Tibetan Plateau in the general circulation, *Meteorol. Atmos. Phys.*, 67, 181–198, doi:10.1007/BF01277509, 1998.
- 5 Ye, H., Zhang, R., Shi, J., Huang, J., Warren, S. G., and Fu, Q.: Black carbon in seasonal snow across northern Xinjiang in northwestern China, *Environ. Res. Lett.*, 7, 044002, doi:10.1088/1748-9326/7/4/044002, 2012.
- Yeh, T., Lo, S., and Chu, P.: The wind structure and heat balance in the lower troposphere over Tibetan Plateau and its surrounding, *Acta Meteorol. Sin.*, 28, 108–121, 1957.
- 10 Zhang, R., Hegg, D. A., Huang, J., and Fu, Q.: Source attribution of insoluble light-absorbing particles in seasonal snow across northern China, *Atmos. Chem. Phys.*, 13, 6091–6099, doi:10.5194/acp-13-6091-2013, 2013.
- Zhang, X. Y., Arimoto, R., Cao, J. J., An, Z. S., and Wang, D.: Atmospheric dust aerosol over the Tibetan Plateau, *J. Geophys. Res.*, 106, 18471–18476, 2001.
- 15 Zhao, L., Ping, C., Yang, D., Cheng, G., Ding, Y., and Liu, S.: Changes of climate and seasonally frozen ground over the past 30 years in Qinghai-Xizang (Tibetan) Plateau, China, *Global Planet. Change*, 43, 19–31, 2004.
- Zhao, S., Ming, J., Xiao, C., Sun, W., and Qin, X.: A preliminary study on measurements of black carbon in the atmosphere of northwest Qilian Shan, *J. Environ. Sci.*, 24, 152–159, doi:10.1016/S1001-0742(11)60739-0, 2012.
- 20 Zhao, Z., Cao, J., Shen, Z., Xu, B., Chen, L.-W. A., Ho, K., Han, Y., Zhu, C., and Liu, S.: Aerosol particles at a high-altitude site on the Southeast Tibetan Plateau, China: implications for pollution transport from South Asia, *J. Geophys. Res.-Atmos.*, 118, 11360–11375, doi:10.1002/jgrd.50599, 2013.

Black carbon over the Himalayas and Tibetan Plateau

R. Zhang et al.

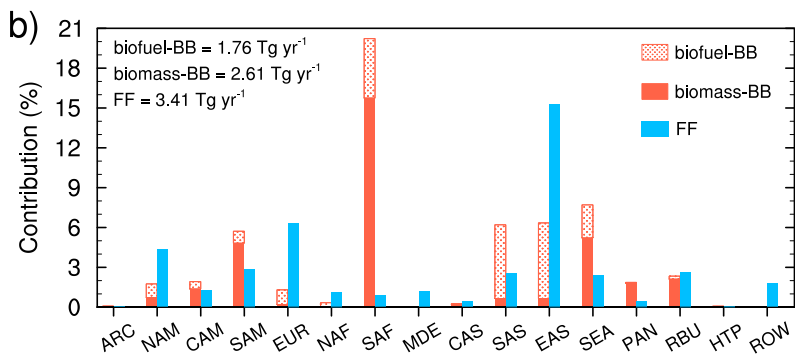
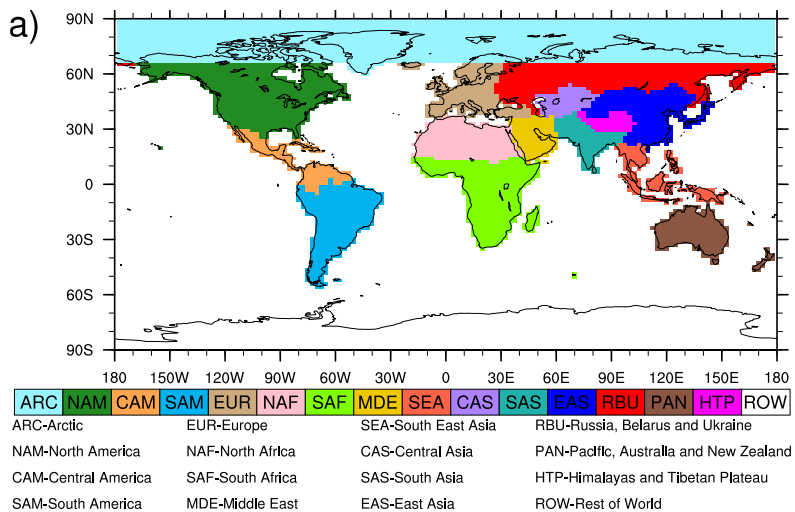


Figure 1. (a) Tagged source regions and (b) the respective percentage contributions to global annual mean BC emissions from the individual source regions and sectors (including biofuel, biomass burning and fossil fuel). The global annual mean BC emission rate is 7.78 Tg yr^{-1} , which is divided up into the three sectors as indicated by the numbers at the upper-left corner.

Title Page

Abstract Introduction

Conclusions References

Tables Figures

◀ ▶

◀ ▶

Back Close

Full Screen / Esc

Printer-friendly Version

Interactive Discussion



Black carbon over the Himalayas and Tibetan Plateau

R. Zhang et al.

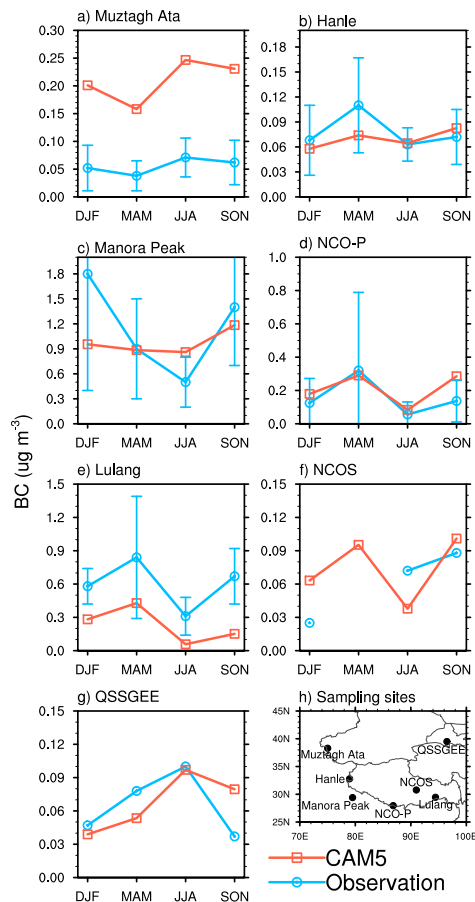


Figure 2. Seasonal mean surface BC aerosol concentration ($\mu\text{g m}^{-3}$) from observations (blue lines with error bars denoting SD) and CAM5 simulation (red lines) at the seven sampling sites listed in Table 1 and marked in map of (h).

Title Page

Abstract Introduction

Conclusions References

Tables Figures

◀ ▶

◀ ▶

Back Close

Full Screen / Esc

Printer-friendly Version

Interactive Discussion



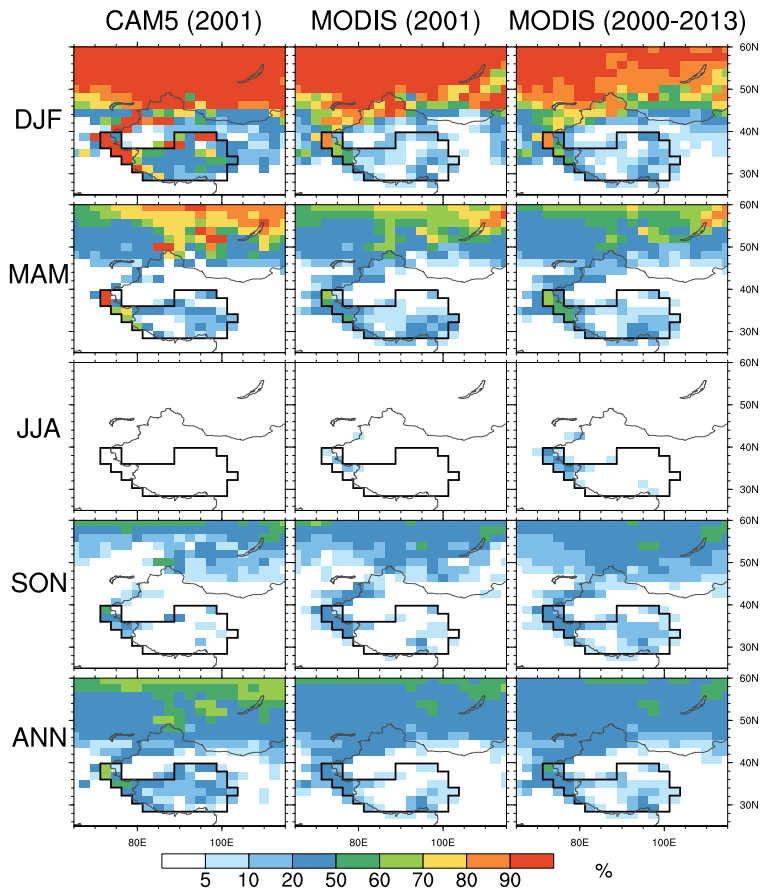


Figure 3. Seasonal and annual mean snow cover fraction from CAM5 simulation for year 2001 (left), and MODIS retrieval for 2001 (middle) and 2000–2013 (right). The summer (JJA) in 2001 for both CAM5 and MODIS only includes July and August due to missing MODIS data in June. The HTP region is marked with black outline.

Black carbon over the Himalayas and Tibetan Plateau

R. Zhang et al.

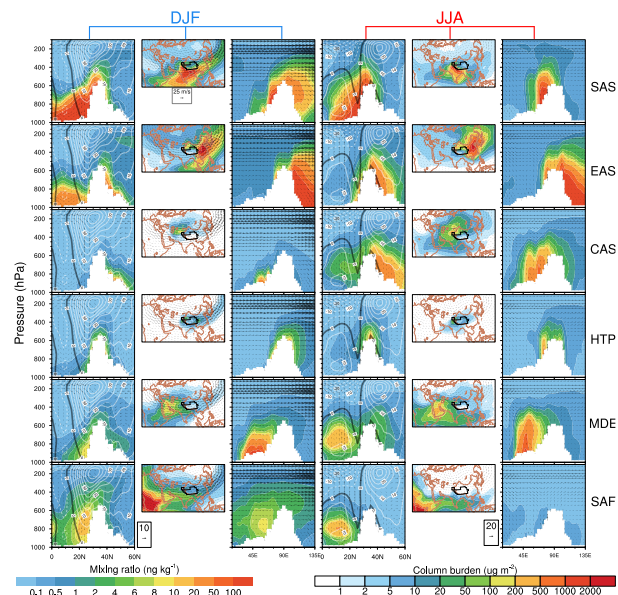


Figure 4. The first column shows the latitude-height distributions of DJF BC mass mixing ratios (in ng kg^{-1} , colors) averaged over $71.25\text{--}101.25^\circ\text{E}$, originating from BB and FF sectors in the tagged source regions (corresponding to different rows); the white shaded area denotes topography, and the superimposed white contours at intervals of 5 m s^{-1} represent the westerly (solid) and easterly (dashed) DJF mean zonal winds along the cross-section with the thick solid black contour at 0 m s^{-1} ; the wind vectors (consisting of vertical velocity in units of $-10^{-4}\text{ hPa s}^{-1}$ and meridional wind in m s^{-1}) are represented by arrows. Colors in the second column denote spatial distribution of the DJF mean BC column burden (in $\mu\text{g m}^{-2}$), originating from different source regions, and the arrows represent the DJF mean horizontal wind vectors at 500 hPa; the HTP is marked with black outline. The third column is similar to the first column except that the quantities are on the longitude-height cross-section averaged over $28\text{--}40^\circ\text{N}$, and thus the horizontal component of the wind vectors is zonal wind (m s^{-1}) instead. The fourth to sixth columns are the same as the first to third columns, respectively, but for JJA means instead.



Back

Close

Full Screen / Esc

Printer-friendly Version

Interactive Discussion



Black carbon over the Himalayas and Tibetan Plateau

R. Zhang et al.

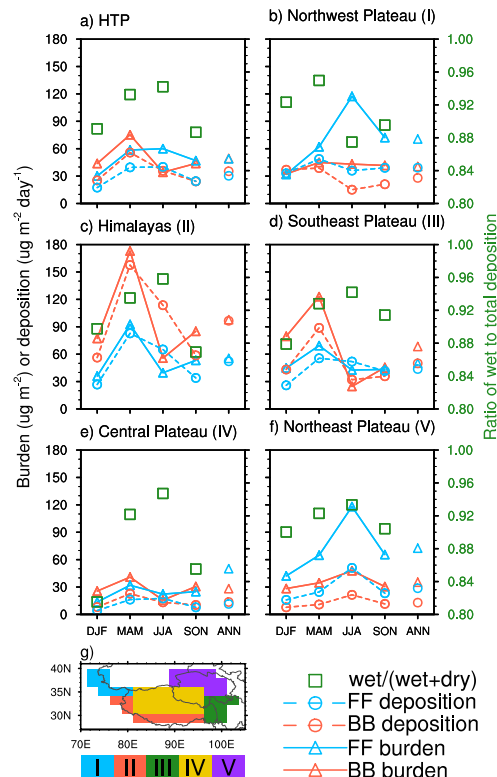


Figure 5. Seasonal and annual mean BC column burden (solid lines and open triangles, in $\mu\text{g m}^{-2}$) and deposition rate (dashed lines and open circles, in $\mu\text{g m}^{-2} \text{ day}^{-1}$) over **(a)** the HTP, **(b)** Northwest Plateau, **(c)** Himalayas, **(d)** Southeast Plateau, **(e)** Central Plateau and **(f)** Northeast Plateau, emitted from BB (red color) and FF (blue color) source sectors. The green squares denote the ratio of wet to total BC deposition (using y axis on the right) in four seasons over each receptor region. The geographical locations of five sub-regions of HTP are indicated in **(g)**.



Back

Close

Full Screen / Esc

Printer-friendly Version

Interactive Discussion



Black carbon over the Himalayas and Tibetan Plateau

R. Zhang et al.

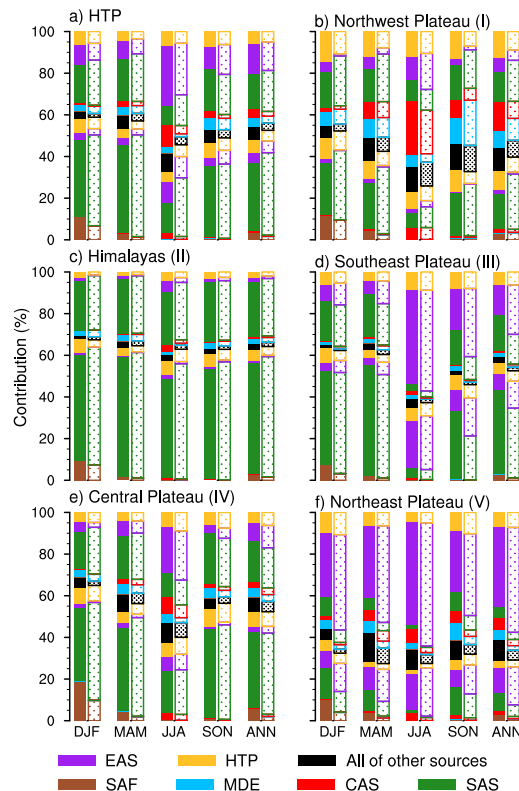


Figure 6. Fractional contributions (measured by the lengths of color bars) to seasonal and annual mean BC column burden (solid pattern bars) and deposition (dotted pattern bars) over **(a)** the HTP, **(b)** Northwest Plateau, **(c)** Himalayas, **(d)** Southeast Plateau, **(e)** Central Plateau, and **(f)** Northeast Plateau, originating from six major tagged source regions (indicated by colors at the bottom) for BB (colors below the black bar) and FF (colors above the black color) emissions. The black bar in each column represents the contribution from all of the other tagged source regions and sectors.

Title Page

Abstract Introduction

Conclusions References

Tables Figures

◀ ▶

◀ ▶

Back Close

Full Screen / Esc

Printer-friendly Version

Interactive Discussion



Black carbon over the Himalayas and Tibetan Plateau

R. Zhang et al.

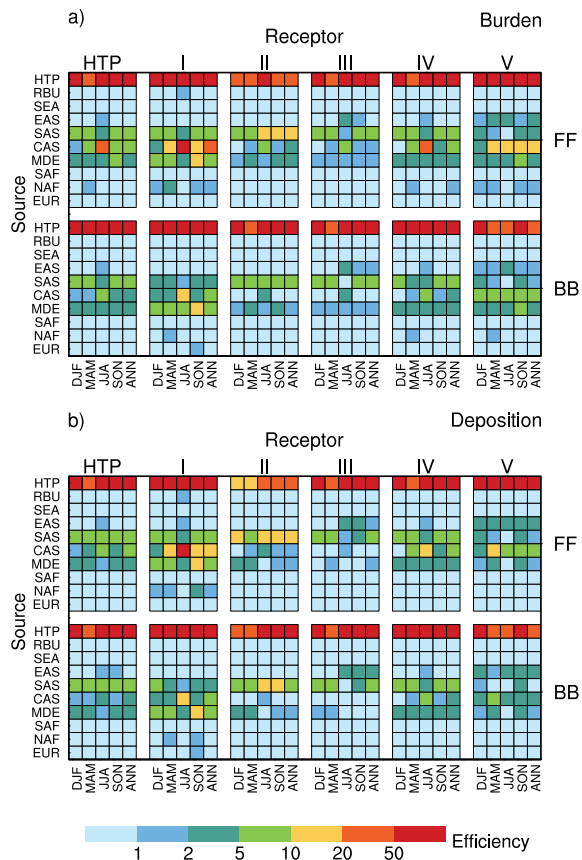


Figure 7. Efficiency of FF (top) and BB (bottom) emissions from ten source regions (on the y axis) in changing seasonal and annual mean (a) BC column burden and (b) deposition over the HTP and each of the five sub-regions: Northwest Plateau (I), Himalayas (II), Southeast Plateau (III), Central Plateau (IV) and Northeast Plateau (V).

Title Page

Abstract Introduction

Conclusions References

Tables Figures

◀ ▶

◀ ▶

Back Close

Full Screen / Esc

Printer-friendly Version

Interactive Discussion



Black carbon over the Himalayas and Tibetan Plateau

R. Zhang et al.

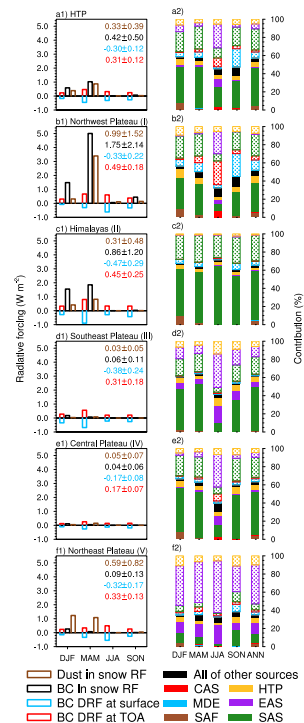


Figure 8. Seasonal mean radiative forcing (left column) induced by the various BC effects (indicated by the color legend at the bottom) and dust-in-snow effect over (a1) the HTP, (b1) Northwest Plateau, (c1) Himalayas, (d1) Southeast Plateau, (e1) Central Plateau and (f1) Northeast Plateau. The corresponding annual mean forcings and one SD (for 12 monthly means) are shown in numbers on the top-right corner of each panel. The right column (a2–f2) panels represent source contribution to surface BC-in-snow radiative forcing over the corresponding receptors from tagged source regions (colors) and sectors (solid pattern bar and dotted pattern bar for BB and FF, respectively). The black bar in each column represents the contribution from all of the other tagged source regions and sectors.